

## DETAILED ONE-DIMENSIONAL ANALYSIS OF SUGARCANE BAGASSE GASIFICATION PROCESS IN BUBBLING FLUIDIZED BEDS

Andrés B. Villamil Castellanos, villamil@ufrj.br

Jean M. de Pinho, jean.pinho@ufrj.br

Albino J. K. Leiroz\*, leiroz@mecanica.coppe.ufrj.br

Manuel E. C. Cruz, manuel@mecanica.coppe.ufrj.br

Department of Mechanical Engineering  
Federal University of Rio de Janeiro  
PO Box 68503 – Rio de Janeiro, RJ, Brazil – 21941-972

**Abstract.** Computational simulations of sugarcane bagasse gasification are conducted to evaluate the sensitivity of the process to the change of selected gasification parameters. A commercial code is used to obtain results for an atmospheric bubbling fluidized bed gasifier. The code is based on phenomenological models and considers the process one-dimensional. Axial profiles of concentration and temperature in the reactor, obtained for different values of the air/fuel ratio, are presented and analyzed. The simulation results follow the trends observed in real processes of biomass gasification in bubbling fluidized beds.

**Keywords:** Gasification, biomass, sugarcane bagasse, fluidized bed, simulation, CeSFaMB™.

### 1. NOMENCLATURE

F	Mass flow	$\frac{\text{kg}}{\text{s}}$
SR	Stoichiometric ratio	--
LHV	Syngas low heating value	$\frac{\text{MJ}}{\text{kg}}$
$T_{av,B}$	Average bed temperature	K

#### Greek letters

$\eta$	Equipment efficiency	--
--------	----------------------	----

#### Subscripts

fuel	Sugarcane bagasse	--
air	Air	--

### 2. INTRODUCTION

Biomass is a renewable source of energy and organic carbon. The use of biomass as fuel offers some advantages, not only in terms of energy, but also in economical, political, environmental and social terms. The conversion of biomass into energy can be accomplished following a variety of processes. Gasification has been identified as one of the most promising areas of research and development for the conversion of biomass into energy.

Gasification is a process where raw material in liquid or solid form is converted into a gaseous product that can be used for energy release purposes in other applications such as reciprocating engines and turbines or use as feedstock for the production of other chemical products. The gasification of biomass in fluidized bed reactors has advantages of presenting a nearly isothermal condition within the solid bed and allowing favorable condition for process control and scale up.

In some tropical countries, sugarcane is the main raw material to the production of ethanol and sugarcane bagasse has become a major waste byproduct of this process. Currently, it is used, mainly, as fuel in combustion processes associated with steam cycles. However, the use of as fuel only allows the usage of 30% of the energy of the biomass, whereas the gasification allows the usage of between 75% and 80% of that energy (Galip and Jordan, 2011).

Mathematical models are useful in designing, in predicting the behavior and in analyzing the effects of the process parameters on gasifier performance. In this work, simulations made with the commercial code CeSFaMB™ of

---

\* Author to whom correspondence should be addressed.

sugarcane bagasse gasification in bubbling fluidized bed with different values of air/fuel ratios are presented and analyzed.

### 3. BASIS OF THE MODEL

Gómez-Barea e Leckner (2010) defines three types of mathematical models for the description of gasification in bubbling fluidized beds: black box model, fluidization models and CFD models. Fluidization models are a compromise between simplicity and accuracy, since the momentum equations are not solved. Instead, two or more phases are defined in the bed and the flow pattern of each phase is described by semi-empirical correlations of fluidization models.

The basic model used by CeSFaMB<sup>TM</sup> is based in the fluidization theory. The equipment is divided in two main regions: bed and freeboard. The bed is formed by two phases: emulsion and bubble. The emulsion contains all of the solids of the bed and a fraction of gas, whereas the bubbles are formed only by gas. The heat and mass transport between phases is modeled with semi-empirical correlations, as shown in Souza-Santos (2004).

Some simplifications, based in operational conditions and equipment characteristics, are introduced in the model. Some of the most important simplifications are related to steady-state regime and one-dimensional flow assumptions. Other basic assumptions of the CeSFaMB<sup>TM</sup> model, along with detailed associated explanations, are discussed in Souza-Santos (2004) and Souza-Santos (2007).

For the CeSFaMB<sup>TM</sup> model mass and energy conservation equations are defined for the bed and the freeboard. In the bed, the mass and energy conservation are applied to the emulsion and bubble phases, separately. The species balance for the bubble gases is given as,

$$\frac{dF_{i,b}}{dz} = R_{hom,b,i} \frac{dV_b}{dz} - f_{b-ge,i} \frac{dA_b}{dz} \quad (1)$$

where  $F_{i,b}$  is the mass flow of the chemical specie  $i$  in the bubble;  $R_{hom,b,i}$  is the rate of generation or consumption of the chemical specie  $i$  by homogeneous chemical reaction in the bubble;  $V_b$  is the volume of the bubble;  $f_{b-ge,i}$  is the mass flux of the chemical specie  $i$  between bubble and emulsion phase and  $A_b$  is the surface area of the bubble. The species balance for the emulsion gases are written as

$$\frac{dF_{i,ge}}{dz} = \sum_{m=1}^3 R_{het,se,i} \frac{dA_{se,m}}{dz} + R_{hom,ge,i} \frac{dV_{ge}}{dz} + f_{b-ge,i} \frac{dA_b}{dz} \quad (2)$$

where  $F_{i,ge}$  is the mass flow of the chemical specie  $i$  in the gas of the emulsion phase;  $R_{het,se,i}$  is the rate of generation or consumption of the chemical specie  $i$  by heterogeneous chemical reaction between the gas and solid in the emulsion phase. Note that  $m$  represent each type of solid present in the bed ( $m=1$ , carbonaceous;  $m=2$ , limestone or dolomite;  $m=3$ , inert) (Souza-Santos, 2004).  $R_{hom,ge,i}$  is the rate of generation or consumption of the chemical species  $i$  by chemical homogeneous reaction in the gas of the emulsion phase;  $V_{ge}$  is the volume of the gas of the emulsion. The species balance for the solids in the bed is given as

$$F_{m,in,B} - F_{m,out,B} = \int_0^{z_B} \sum_{m=1}^3 R_{het,se,i} \frac{dA_{se,m}}{dz} dz \quad (3)$$

where  $F_{m,in,B}$  is the mass flow of solids type  $m$  entering in the bed;  $F_{m,out,B}$  is the mass flow of solids type  $m$  leaving the bed.

The energy conservation equation in the bubble phase is written as

$$F_b c_b \frac{dT_b}{dz} = [R_{Q,b} - R_{C,b-ge} - R_{h,b-ge}] \frac{dV_b}{dz} \quad (4)$$

where  $F_b$  is the mass flow of gas in the bubble;  $c_b$  is the specific heat at constant pressure;  $T_b$  is the temperature in the bubble;  $R_{Q,b}$  rate of energy generation or consumption due to chemical reactions;  $R_{C,b-ge}$  is the rate of energy transfer from the bubble to the gas of the emulsion phase due to convection; and  $R_{h,b-ge}$  is the rate of energy transfer from the bubble to the gas of the emulsion phase due to mass transfer between phases.

For the emulsion gas, the energy conservation equation is written as

$$F_{ge} c_{ge} \frac{dT_{ge}}{dz} = \left[ -R_{Q,ge} + (R_{C,b-ge} + R_{h,b-ge}) \frac{dV_b/dz}{dV_{ge}/dz} - R_{C,ge-W} + \sum_{m=1}^3 (R_{C,ge-se,m} + R_{h,ge-se,m}) \right] \frac{dV_{ge}}{dz} \quad (5)$$

where  $F_{ge}$  is the mass flow of gas in the emulsion phase;  $c_{ge}$  is the specific heat at constant pressure;  $T_{ge}$  is the temperature of the gas in the emulsion phase;  $R_{Q,ge}$  is the rate of energy generation or consumption due to chemical reactions in the gas of the emulsion phase;  $R_{C,ge-se,m}$  is the rate of energy transfer from the gas of the emulsion phase to the solid type  $m$  due to convection; and  $R_{h,ge-se,m}$  is the rate of energy transfer from the gas of the emulsion phase to the solid type  $m$  due to mass transfer.

For the solid in the gasifier bed, the energy conservation equation is written as

$$F_{F,m} c_{se,m} \frac{dT_{se,m}}{dz} = \left[ -R_{Q,se,m} + (R_{C,ge-se,m} - R_{h,ge-se,m}) \frac{dV_{ge}/dz}{dV_{se,m}/dz} - \sum_{n=1}^3 (R_{R,se,m-se,n} - R_{C,se,m-se,n}) \right] \frac{dV_{se,m}}{dz} \quad (6)$$

where  $F_{F,m}$  is the circulation rate of solid  $m$  in the bed;  $T_{se,m}$  is the temperature of solid type  $m$ ;  $R_{Q,se,m}$  rate of energy generation or consumption due to heterogeneous chemical reactions;  $R_{R,se,m-se,n}$  is the rate of energy transfer from solids type  $m$  to solids type  $n$  due to radiation; and  $R_{C,se,m-se,n}$  is the rate of energy transfer from solids type  $m$  to solids type  $n$  due to conduction.

#### 4. EXPERIMENTAL CASE

Campoy (2009) performed experimental tests in a gasification pilot-plant in the University of Sevilla, Spain. Pilot-plant gasification tests were conducted at atmospheric pressure and temperatures within the range of 700-800 °C to assess the technical viability of gasifying untreated olive stones. Different air flow rates and air-to-biomass ratios were used, leading to stoichiometric ratios of 19%, 27% and 35%. Details on the gasifier used and on the experimental operational conditions adopted are found in Campoy (2009) and Gómez-Barea *et al* (2005) and were used to develop a simulation case in CeSFaMB™. Numerical results for molar fractions of the main chemical species in the syngas produced are shown in Tab. 1 for different stoichiometric ratios and compared with experimental data (Campoy, 2009).

Table 1. Experimental and numerical results for molar fractions of main syngas species for different stoichiometric ratios (dry basis).

Chemical species	Stoichiometric Ratio [%]					
	19		27		35	
	Exp.	Num.	Exp.	Num.	Exp.	Num.
H <sub>2</sub>	13,2	20,82	12,6	13,21	8,7	9,18
CO	18,2	20,56	17,6	15,6	15,8	12,30
CO <sub>2</sub>	14,2	13,22	14,9	14,43	15,1	15,45
CH <sub>4</sub>	6,0	5,28	5,2	4,3	5,1	3,28

Results in Tab.1 show a similar qualitative behavior between numerical and experimental results as the stoichiometric ratio varies. Nevertheless, quantitative differences between the results are observed, reaching a maximum (57.7%) for H<sub>2</sub> and a stoichiometric ratio of 19%. For Souza-Santos (2012) the difference is explained from the absence of olive stone properties in the CeSFaMB™ database, leading to the use of generic biomass data for the pyrolysis modeling by the code.

Numerical and experimental average bed temperatures are also be compared, as shown in Tab. 2.

Table 2. Experimental and numerical results for sverage bed temperature for different stoichiometric ratios.

Exp.	Stoichiometric Ratio [%]					
	19		27		35	
	Exp.	Num.	Exp.	Num.	Exp.	Num.
780	775	805	880	812	970	

The average bed temperature increases for higher values of the stoichiometric ratio. As more oxidant is made available for the gasification process, the generated gas combustion within the gasifier is enhanced leading to increases of the amount of CO<sub>2</sub> in the syngas and solid bed temperature, as shown in Tabs.1-2, respectively.

## 5. SIMULATION DETAILS

The equipment considered for the simulations of the present work is a gasification pilot plant built by PID Eng&Tech and installed in the Petrobras Research Center (CENPES). The gasification plant is constituted by an atmospheric fluidized bed reactor, two cyclones connected in series, a multiple tube heat exchanger used to cool the hot gases and separate the condensed tar and steam, a wet gas scrubber to remove the contaminants and a control system to the main variables of the process, as shown in Fig. 1. The plant can be operated with air and/or steam as gasifying agents and has a continuous feeding system for the biomass.

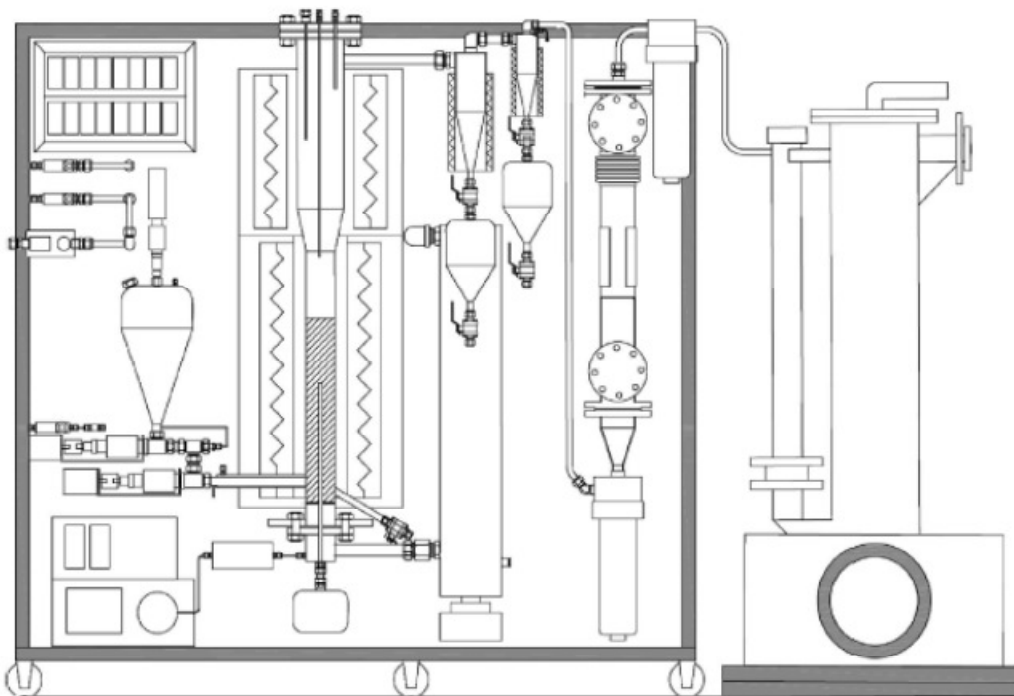


Figure 1. Diagram of the gasification pilot plant (PID Eng&Tech).

The basic geometry of the gasifier is shown in Tab. 3. The gas distributor of gasifier is a porous plate with a 150 microns mesh and is placed at the bottom of the reactor.

Table 3. Basic geometry of the gasifier.

Internal diameter [m]	Respective axial position of the diameter [m]
0.0828	0.000
0.0828	0.585
0.1340	0.897
0.1340	1.305

Four and a half kilograms of sand pre-heated to 400 °C are used as inert bed material. The particle size distribution of the inert particles and sugarcane bagasse are shown in Tabs. 4 and 5, respectively. Table 6 shows the ultimate and proximate analyses and the high heating value for the sugarcane bagasse. The mass flow of sugarcane bagasse fed into the gasifier is  $2.78 \times 10^{-4}$  kg/s.

Air at 400 °C and 120 kPa enters in the equipment through the distributor. Different air mass flows rates, corresponding to 20%, 25% and 30% of the theoretical air, are considered in the present work.

Table 4. Particle size distribution of inert particles.

Sieve opening [mm]	Retained mass [%]
0.000	0.01
0.045	9.93
0.120	16.14
0.175	12.05
0.250	19.59
0.363	15.98
0.463	6.40
0.550	7.03
0.725	9.73
0.850	3.14

Table 5. Particle size distribution of sugarcane bagasse.

Mesh number	Retained mass [%]
10	0.005
18	0.005
35	0.830
60	2.100
120	43.170
230	31.000
400	22.890

Table 6. Ultimate and proximate analysis of sugarcane bagasse.

Ultimate analysis	%	Proximate analysis	%
C	47.63	Moisture	4.26
H	6.16	Volatile	77.99
O	38.46	Fixed Carbon	11.03
N	0.42	Ash	6.72
S	0.31		
Ash	7.02	<b>HHV [MJ/kg]</b>	16.73

The study was conducted using four different sugarcane bagasse mass flows and three stoichiometric ratios. Table 7 shows the air mass flow for each sugarcane bagasse feeding rate and stoichiometric ratio considered.

Table 7. Air mass flows used in the simulations.

Sugarcane bagasse mass flow [kg/h]	Stoichiometric Ratio [%]		
	25	30	35
1.0	0.000395	0.000474	0.000553
0.8	0.000316	0.000379	0.000442
0.6	0.000237	0.000284	0.000332
0.4	0.000158	0.000190	0.000221

## 6. RESULTS

Figure 2 shows the molar fraction profiles of CO<sub>2</sub>, CO and O<sub>2</sub> and the molar fraction profiles of H<sub>2</sub>O, H<sub>2</sub> and CH<sub>4</sub> along the gasifier bed for a stoichiometric ratio of 25% and 1,0 kg/h of sugarcane bagasse entering in the gasifier. Note that oxygen is totally consumed at the bottom of the bed due the oxidation reactions, increasing the concentrations of CO<sub>2</sub> and H<sub>2</sub>O. For downstream positions, the concentrations of CO and H<sub>2</sub> increase due to the pyrolysis process and the absence of oxygen with an increasing of the water-gas shift reaction rate (Basu, 2010; Souza-Santos, 2004).

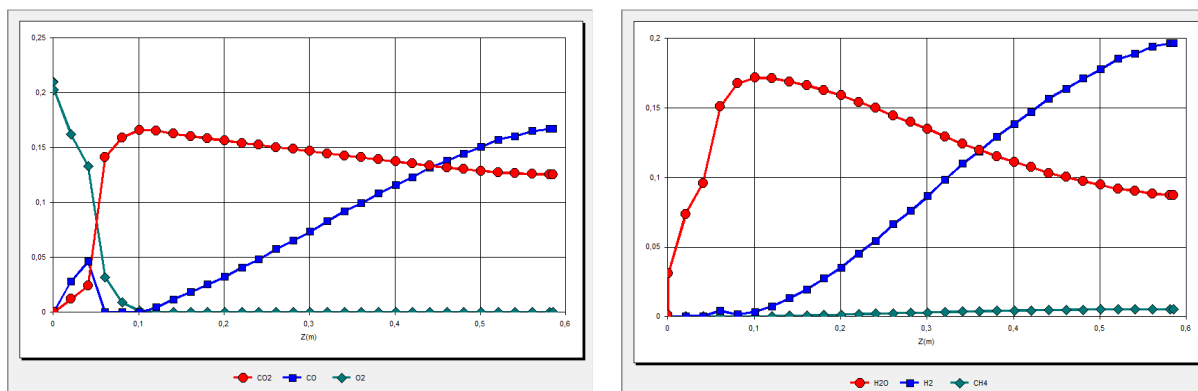


Figure 2. Molar fraction profiles in the bubbles of CO<sub>2</sub>, CO, O<sub>2</sub> (left), H<sub>2</sub>O, H<sub>2</sub> and CH<sub>4</sub> (right) in the bed (SR = 25% and F<sub>fuel</sub> = 1.0 kg/h).

Figure 3 shows the temperature profile along the gasifier bed for a stoichiometric ratio of 25% and 1,0 kg/h of sugarcane bagasse entering in the gasifier. The rapid increase in the bubble temperature may be attributed to the exothermic oxidation reactions in the lower part of the reactor. It is noteworthy that at the sugarcane bagasse feeding point ( $z = 0.07$  m) the rate of temperature increase reaches a maximum. Following oxygen depletion, results show that temperature decreases to an approximate constant value of 950 K due to the endothermic homogeneous and gasification reactions.

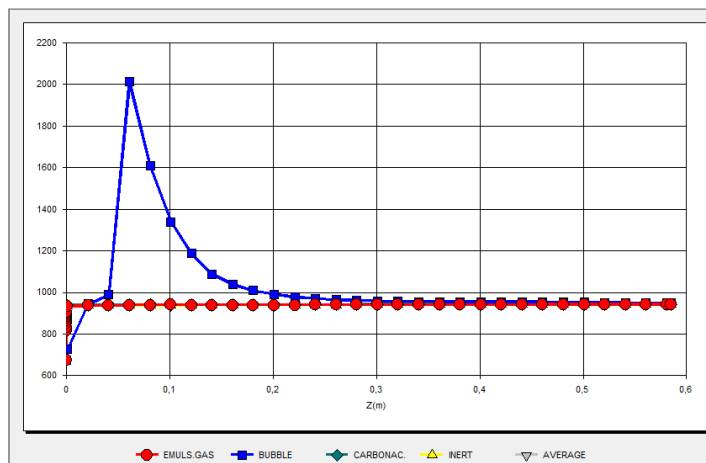


Figure 3. Temperature profile of the bed (SR = 25% and  $F_{fuel} = 1.0$  kg/h).

A compilation of the obtained results for the sugarcane bagasse feeding rates and stoichiometric ratios considered are shown in the Tab. 8. The results are expressed in terms of syngas composition and heating value. Results for average bed temperature and equipment efficiency, defined as the ratio of enthalpy leaving the gasifier with the syngas to the enthalpy of the biomass, are also shown in Tab.8.

Table 8. Main results of the study.

Operational conditions												
$F_{fuel}$ [kg/h]	1.0	1.0	1.0	0.8	0.8	0.8	0.6	0.6	0.6	0.4	0.4	0.4
$F_{air}$ [kg/h]	1.4	1.7	2.0	1.1	1.4	1.6	0.8	1.0	1.2	0.6	0.7	0.8
Analysis variables												
SR	25	30	35	25	30	35	25	30	35	25	30	35
Syngas composition (molar fraction)												
H <sub>2</sub>	21.6	18.0	15.3	22.1	18.5	15.6	21.5	19.2	16.2	24.0	19.9	16.9
H <sub>2</sub> O	7.9	9.7	11.3	7.5	9.0	10.6	7.6	8.6	9.9	5.7	7.7	8.9
CO	18.2	15.7	13.8	17.3	15.2	13.4	16.0	14.6	12.7	15.6	13.4	11.8
CO <sub>2</sub>	12.3	12.7	12.9	13.1	13.2	13.3	14.0	14.0	14.0	14.9	15.0	15.0
CH <sub>4</sub>	0.5	0.3	0.0	0.5	0.4	0.2	0.5	0.4	0.3	0.4	0.4	0.3
Process variables												
LHV [MJ/kg]	5.0	4.1	3.4	5.0	4.1	3.4	4.7	4.1	3.4	4.8	4.0	3.4
$\eta$	73.3	65.6	57.6	72.1	66.2	59.2	68.4	66.6	59.9	71.4	65.4	60.4
$T_{av,B}$ [K]	939	999	1044	915	969	1013	872	923	969	808	863	902

Results in Tab.8 show that the syngas produced at higher stoichiometric ratio conditions presents a lower heating value due to enhanced partial oxidation of the produced gas within the equipment. Since the oxidation reaction is exothermic, higher solid bed average temperatures are also observed for higher stoichiometric ratio conditions. The average time for completing a case simulation is 30 minutes.

## 7. CONCLUSIONS

Computational simulations of sugarcane bagasse gasification are conducted to evaluate the sensitivity of the process to the change of selected gasification parameters. The commercial code is validated with literature data and used to the efficiently simulate the gasification process in a bubbling fluidized bed reactor. The obtained numerical results are in

qualitative accordance with the real behavior of the gasification process. Further comparisons with experimental data are required in order to evaluate the quantitative characteristics of the numerical results obtained.

## 8. ACKNOWLEDGEMENTS

The authors gratefully acknowledge the support provided by CENPES/ Petrobras in the development of the present work. M. E. Cruz gratefully acknowledges the financial support from the Brazilian science fostering agencies CNPq (Grants PQ-302725/2009-1 and Univ-470306/2010-6) and FAPERJ (Grant CNE-E-26/103.058/2011).

## 9. REFERENCES

- Basu, P., 2010. "Biomass Gasification and Pyrolysis. Practical Design". Elsevier Burlington. USA.
- Campoy, M., 2009, "Gasificación de biomasa y residuos en lecho fluidizado: Estudios en planta piloto." Tesis de D. Sc. Universidad de Sevilla, Sevilla, España.
- Galip, A., Jordan, C.A., 2011. "Gasification of fuel cane bagasse in downdraft gasifier: Influence of Lignocellulosic composition and fuel particle size on syngas composition and yield". *Energy and Fuels*, Vol. 25, pp. 2274–2283.
- Gómez-Barea, A.; Arjona, R.; Ollero, P., 2005 "Pilot-Plant Gasification of Olive Stone: A Technical Assesment." *Energy and Fuels*. Vol. 19 (2). pp. 598-605.
- Gómez-Barea, A., Leckner, B., 2010. "Modeling of biomass gasification in fluidized bed". *Progress in Energy and Combustion Science*, Vol. 36, pp. 444–509.
- PID Eng&Tech, "Gasification pilot plant. Automated and computerized laboratory-pilot plant for the study of gasification process". < <http://www.pidengtech.com/documents/GASIFICATION/gasificationBrochure.pdf>>.
- Souza-Santos, M.L., 2004. "Solid Fuels Combustion and Gasification. Modeling, Simulation, and Equipment Operation". Marcel Dekker, Inc. USA.
- Souza-Santos, M.L., 2007. "A new version of CSFB, comprehensive simulator for fluidised bed equipment". *Fuel*, Vol. 86, pp. 1684–1709.
- Souza-Santos, M.L., 2012 "CeSFaMB™/CSFMB®. Comprehensive Simulator of Fluidized and Moving Bed Equipment. Series 53". 405 pp.

## 10. RESPONSIBILITY NOTICE

The authors are the only responsible for the printed material included in this paper.